Published online 01 April 2014 *Nucleic Acids Research, 2014, Vol. 42, No. 9* ***5863–5870***
doi: 10.1093/nar/gku238

Dissecting the chemical interactions and substrate structural signatures governing RNA polymerase II trigger loop closure by synthetic nucleic acid analogues

Liang Xu[1], Kyle Vincent Butler[2], Jenny Chong[1], Jesper Wengel[3], Eric T. Kool[2] and Dong Wang[1,*]

[1]Skaggs School of Pharmacy and Pharmaceutical Sciences, The University of California, San Diego, La Jolla, CA 92093–0625, USA, [2]Department of Chemistry, Stanford University, Stanford, CA 94305–5080, USA and [3]Nucleic Acid Center and Biomolecular Nanoscale Engineering Center, Department of Physics, Chemistry and Pharmacy, University of Southern Denmark, Campusvej 55, 5230 Odense M, Denmark

Received February 3, 2014; Revised March 07, 2014; Accepted March 10, 2014

ABSTRACT

The trigger loop (TL) of RNA polymerase II (Pol II) is a conserved structural motif that is crucial for Pol II catalytic activity and transcriptional fidelity. The TL remains in an inactive open conformation when the mismatched substrate is bound. In contrast, TL switches from an inactive open state to a closed active state to facilitate nucleotide addition upon the binding of the cognate substrate to the Pol II active site. However, a comprehensive understanding of the specific chemical interactions and substrate structural signatures that are essential to this TL conformational change remains elusive. Here we employed synthetic nucleotide analogues as 'chemical mutation' tools coupling with α-amanitin transcription inhibition assay to systematically dissect the key chemical interactions and structural signatures governing the substrate-coupled TL closure in *Saccharomyces cerevisiae* Pol II. This study reveals novel insights into understanding the molecular basis of TL conformational transition upon substrate binding during Pol II transcription. This synthetic chemical biology approach may be extended to understand the mechanisms of other RNA polymerases as well as other nucleic acid enzymes in future studies.

INTRODUCTION

RNA polymerase II (Pol II) is the central enzyme responsible for synthesizing mRNA in a highly rapid and accurate manner (1–7). The Pol II trigger loop (TL), an evolutionarily conserved mobile structural motif, plays important roles in controlling high Pol II catalytic activity and transcriptional fidelity (8–15). During Pol II transcription, the nucleoside triphosphate (NTP) substrate first diffuses into an entry (or pre-insertion) site nearby the active site of Pol II elongation complex (EC), where Pol II is in a post-translocation state and its TL is in an inactive open conformation (8,16–18). The correct NTP further moves into the insertion site to assemble correct Watson–Crick base pair with the template base, and subsequently the TL undergoes conformational transition from an inactive open state to a closed active state. This closure of the TL is important for efficient and accurate nucleotide addition (TL-dependent nucleotide addition) (8–15). Finally, following the pyrophosphate ion release and the re-opening of the TL, Pol II translocates from a pre-translocation state to a new post-translocation state for the next round of NTP binding and addition (19). In contrast to the correct substrate binding, TL fails to reach an active closed state when the incorrect substrate (a mismatch in nucleobase or sugar) is bound. This incorrect substrate will either dissociate from the Pol II active site or become misincorporated in a slow and inaccurate manner (TL-independent nucleotide addition)(Figure 1A) (8,9).

α-Amanitin is a specific and potent inhibitor for Pol II transcription. Previous structural studies have revealed that α-amanitin can bind near the Pol II active site and trap the TL in an open inactive conformation. Therefore, α-amanitin prevents the TL from reaching an active closed conformation and greatly reduces the rate of TL-dependent nucleotide addition of cognate substrate by a factor of hundreds (8,9,13,20,21). In sharp contrast, α-amanitin treatment does not significantly affect the incorporation rate of a mismatched substrate, since nucleotide misincorporation proceeds in a TL-independent manner (slow and low fi-

*To whom correspondence should be addressed. Tel: +1 858 822 5561; Fax: +1 858 822 1953; Email: dongwang@ucsd.edu

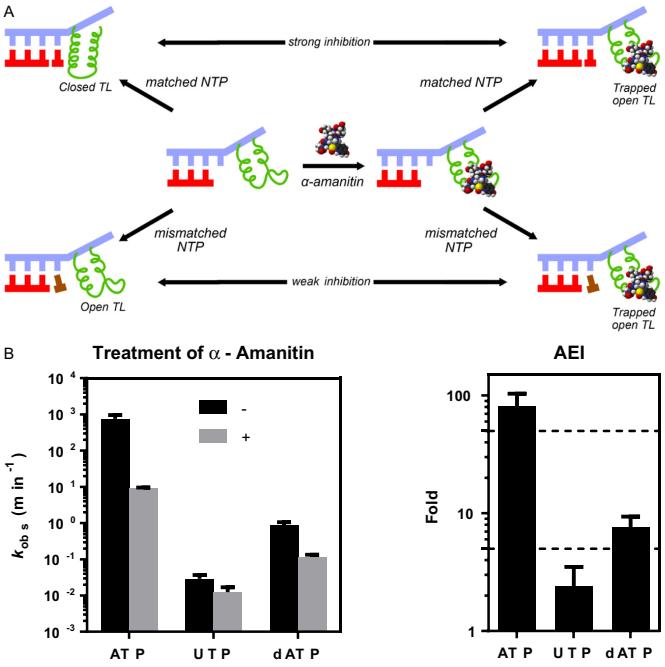

Figure 1. The trigger loop of RNA Pol II promotes correct NTP incorporation and its action is inhibited by α-amanitin. (A) The TL is involved in nucleotide incorporation. (B) α-Amanitin exhibits distinct inhibitory behaviors in different nucleotide incorporation. The left panel presents observed kinetic rates in the absence (−) and presence (+) of α-amanitin; the right panel presents the rate difference affected by α-amanitin, which is calculated by $k_{obs,-}$ (without α-amanitin treatment)/$k_{obs,+}$ (with α-amanitin treatment).

delity) in which the TL is already in an open state. Therefore, the comparison of substrate incorporation rate changes upon α-amanitin treatment provides valuable information about the TL conformational profile upon the binding of any given substrate (Figure 1A). If the TL is able to switch to a closed conformation upon the binding of a given substrate (such as a cognate substrate), one would expect a significant decrease in the substrate incorporation rate with α-amanitin treatment (shifting the dominant TL conformation from a closed conformation to an open conformation). On the other hand, if the TL remains in an open conformation upon the binding of a given substrate (such as a mismatched substrate), one would expect almost no change in the substrate incorporation rate (TL-independent transcription) with α-amanitin treatment. Therefore, the sensitivity of α-amanitin treatment can be used as a measurement of the extent of TL-dependent substrate incorporation of any given substrate.

Previous studies revealed that only the binding of a substrate with matched nucleobase and sugar can trigger the full closure of TL, whereas a substrate with either mismatched nucleobase or sugar cannot (6,8,9,13). However, a detailed understanding of what chemical interactions or structural features govern the conformational transition of TL closure and TL-dependent substrate recognition remains to be elucidated. The nucleobase of matched and mismatched substrates (for example, adenosine triphosphate, ATP, to uridine triphosphate, UTP) are different in multiple ways, including hydrogen-bonding formation and patterns, and the shape and size of the nucleobases. Similarly, a lack of 2′-OH (comparing ribose with deoxyribose) not only results in the loss of hydrogen-bonding capability but also alters the conformation of the sugar ring (from a C3′-endo conformation to C2′-endo conformation) (8,9,22–25). It is not clear what role each factor plays in promoting the TL full closure and TL-dependent transcription. For example, what are the roles of hydrogen bonding between base pairs in promoting the TL closure? What about the base size and stacking? What is the key factor in controlling sugar discrimination?

Dissecting the individual role of a single interaction from the sophisticated interaction network is a difficult task through conventional biology approaches. Here we employed a synthetic nucleic acid chemistry approach to tackle this problem (24,26–33). In this approach, we are able to chemically substitute atoms or functional groups of nucleotides. This ‘chemical mutation’ only changes one structural parameter or one chemical interaction at a time and leaves the rest intact in comparison to canonical nucleotides, allowing us to unravel the individual contribution. Our previous investigations indicate that ‘chemical mutation’ by synthetic chemical biology is an effective way to dissect the individual interactions between Pol II and substrates, which cannot be achieved by conventional observations and analyses (2,34,35). Based on this strategy, we previously used a series of ‘hydrogen-bond-deficient’ analogues to dissect the chemical interactions governing Pol II transcriptional fidelity (34). More recently, by using a sugar ring-disrupted nucleotide analogue, we revealed an unexpected dominant role of sugar integrity in Pol II transcription (35). In the current work, we utilize ‘hydrogen-bond-deficient’ and ‘sugar ring-mutated’ nucleotide analogues as ‘chemical mutation’ tools coupling with α-amanitin transcription inhibition assay to systematically dissect the key chemical interactions and structural signatures governing the substrate-coupled TL conformation closure and shed new light on understanding the molecular basis of TL conformational transition during Pol II transcription.

MATERIAL AND METHODS

Materials

Saccharomyces cerevisiae RNA Pol II was purified as previously described (8,36). The DNA template and non-template oligonucleotides were purchased from IDT. RNA primers were purchased from TriLink Biotechnologies and radiolabelled using [γ-^{32}P]-ATP and T4 Polynucleotide Kinase (NEB). The Pol II ECs for transcription assays were assembled using established methods (34,35,37). RNA primer sequence was 5′-AUCGAGAGGA-3′, the template sequence was 5′-CTACCGATAAGCAGACGXTCCTCTCGATG-3′, where X refers dA or dT, and the non-template strand was 5′-CTGCTTATCGGTAG-3′. All nucleotide analogues (HTP, FTP, LTP, BTP and ITP) were prepared as previously described (38). UNA and LNA were prepared as described (24).

In vitro transcription assays

The Pol II ECs for the transcription assays were assembled using established methods (34,35,37). Briefly, an aliquot of 5′-^{32}P-labeled RNA was annealed with 1.5-fold amount of template DNA and two-fold amount of non-template DNA to form RNA/DNA scaffold in the elongation buffer (20 mM Tris-HCl (pH = 7.5), 40 mM KCl, 5 mM $MgCl_2$). An aliquot of annealed scaffold of RNA/DNA was then incubated with a four-fold excess amount of Pol II at room temperature for 10 min to ensure the formation of a Pol II EC. The Pol II EC is ready for *in vitro* transcription upon mixing with equal volumes of nucleotide solution. Final reaction concentrations after mixing were 25 nM scaffold, 100 nM Pol II, and 1 mM nucleotide in the elongation buffer. Reactions were quenched at various time points by the addition of one volume of 0.5 M ethylenediaminetetraacetic acid (EDTA) (pH = 8.0). The quenched products were analyzed by denaturing polyacrylamide gel electrophoresis (PAGE) and visualized using a storage phosphor screen and Pharos FX imager (Bio-Rad).

Transcription inhibition assays of α-amanitin

In these assays, we used high concentration of α-amanitin (500 mg/L) to make sure that TL-dependent transcription was fully inhibited (9). Briefly, the transcriptional scaffolds were pre-incubated with four-fold amount of Pol II at room temperature for 5 min before the addition of α-amanitin. Next, the mixture was further incubated for another 5 min before incorporation of NTPs. Final reaction conditions were 100 nM Pol II, 25 nM scaffold, 500 mg/L α-amanitin and 1 mM NTP. Reactions were quenched at various time points by the addition of one volume of 0.5 M EDTA (pH = 8.0). Products were separated by denaturing PAGE and analyzed as described above.

Data analysis

Nonlinear-regression data fitting was performed using Prism 6. The time dependence of product formation was fit to a one-phase association (Equation (1)) to determine the observed rate (k_{obs}). The standard deviations of these observed rate constants were derived from three independent kinetic assays:

$$\text{Product} = A\, e^{(-k\text{obs}\, t)} + C. \quad (1)$$

RESULTS

α-Amanitin-induced transcription inhibition as a measurement of the extent of substrate-coupled trigger loop closure

Comparison of substrate incorporation rate changes upon α-amanitin treatment provides a quantitative measurement of the α-amanitin sensitivity for the nucleotide incorporation of any given substrate. Here we defined amanitin effect index (AEI) as a ratio of substrate incorporation rate in the absence of α-amanitin (k_{obs}) over the substrate incorporation rate in the presence of α-amanitin ($k_{obs,\,ama}$). A high AEI ((k_{obs})/($k_{obs,\,ama}$)) value indicates that the given substrate incorporation is highly sensitive to α-amanitin treatment. AEI can provide valuable information about the TL conformational profile upon the binding of any given substrate.

To test whether AEI values could be used as a sensitive indicator of TL conformational transition and the extent of TL-dependent transcription, we performed single nucleotide turnover assays using a defined *in vitro* transcription system (Figure 1B). Here we first focused on measuring the AEI of three well-characterized nucleotides with known TL conformation profiles: cognate substrate (closed TL), mismatched substrate (open TL) and matched deoxyribonucleotide (partially closed TL). We determined that the observed incorporation rate of cognate substrate (ATP for dT template) was ∼750 min^{-1} in the absence of α-amanitin, whereas the substrate incorporation rate dropped to ∼9 min^{-1} in the presence of α-amanitin. The α-amanitin treatment led to an 80–100-fold decrease in the incorporation rate of cognate substrate (AEI = 80–100). In sharp contrast, we only observed a ∼2-fold decline for the incorporation of mismatched UTP for the same dT template upon the α-amanitin treatment (AEI = 2). For matched deoxyribonucleotide incorporation (dATP for dT template), the catalytic rate decreased by ∼10-fold following the treatment with α-amanitin (AEI = 10). These results are fully consistent with the previous biochemical data (8,9,20). Taken together, the distinct AEI values derived from these three substrates provide a convenient and quantitative biochemical characterization of the three distinct states of the TL (closed TL (AEI ∼100), partially closed TL (AEI ∼10), and open TL (AEI ∼1)) (Figure 1B). This AEI system can be extended to test TL conformation and the extent of TL-dependent transcription on any other nucleotides. This defined AEI system also allows us to quantitatively dissect the key chemical interactions and substrate structural signatures governing the substrate-induced TL closure by comparing AEI values for substrate incorporation of these nucleotide analogues with cognate substrate.

Dissecting the role of nucleotide base in TL-dependent transcription

The binding of a substrate with a nucleobase that matches with the DNA template is a prerequisite for TL conformational transition from an open state to a stable closed state, whereas the binding of a substrate with a mismatched nucleobase keeps TL in an open state. To systematically dissect the roles of electrostatic effects (including hydrogen bonding) and steric effects (shape and size) in controlling the TL conformational transition, we used five nonpolar UTP isosteres (denoted by HTP, FTP, LTP, BTP and ITP) that closely mimic the shape of UTP (Figure 2A) (34,39,40). These analogues have been used as effective tools to understand the stacking and steric size effects in some nucleic acid enzymes (34,39,41). Among these five analogues, FTP is nearly identical in both size and shape to UTP. HTP is smaller than UTP, whereas LTP, BTP and ITP are increasingly larger than UTP (with less than 1.0 Å difference in size across the series from HTP to ITP). The nucleotide analogues (such as FTP) are deficient in hydrogen bond formation between base pairs (referred to as the 'hydrogen-bonding deficient' nucleotide analogues) in comparison with the 'wild-type' UTP substrate. These ana-

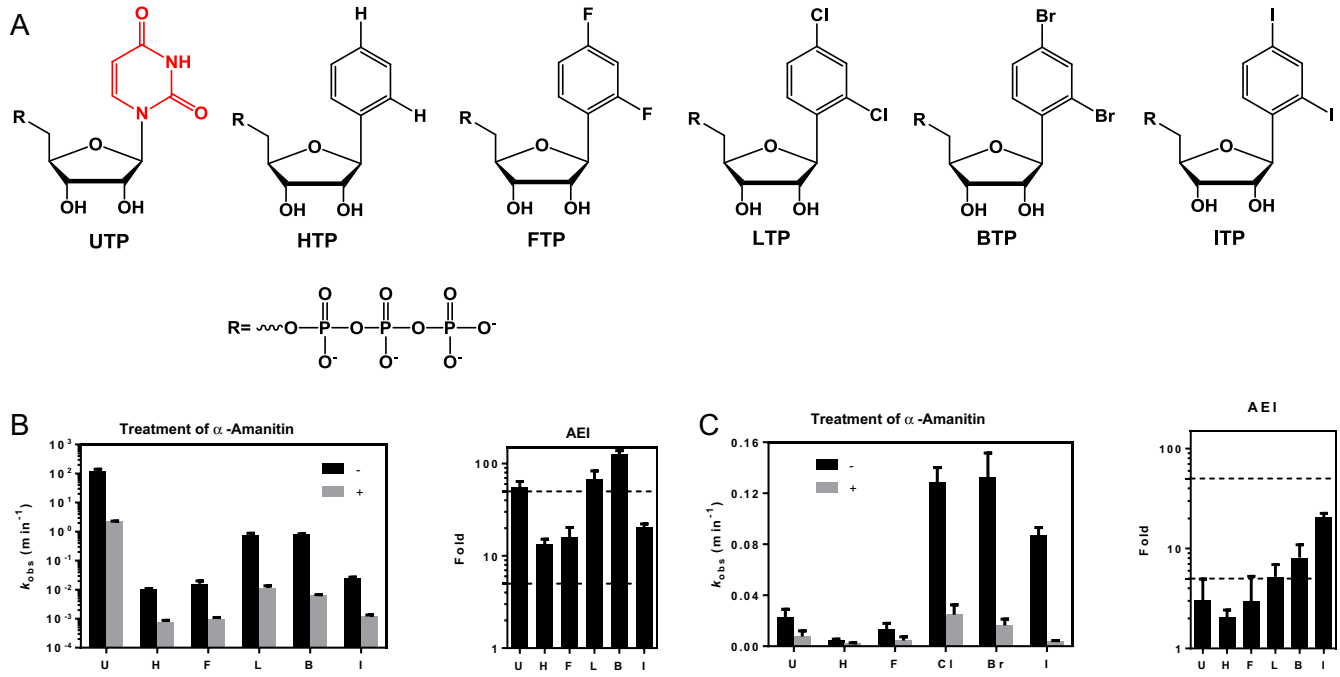

Figure 2. Hydrogen-deficient nucleotide analogues reveal important contributions of base stacking and size fitting to the TL recognition. (A) Nonpolar UTP analogues. (B) Effects of α-amanitin on nucleotide incorporation opposite dA (a matched template). (C) Effects of α-amanitin on nucleotide incorporation opposite dT (a mismatched template). In B and C, the left panel presents observed rates in the absence (−) and presence (+) of α-amanitin; the right panel presents α-amanitin effect index, which is calculated by $k_{obs,-}$ (without α-amanitin treatment)/$k_{obs,+}$ (with α-amanitin treatment).

logues allow us to dissect the individual contributions of hydrogen bonding (FTP versus UTP) as well as size and base stacking effects (comparison among five analogues) in controlling substrate-induced TL closure.

We first measured the respective incorporation rates of UTP and FTP opposite the dA template (matched for UTP incorporation) (Figure 2B and Table 1). The observed incorporation rate of UTP opposite the dA template was very rapid (120 ± 20 min^{-1}), whereas the incorporation rate of the 'hydrogen bonding-deficient' FTP with nearly identical size was greatly reduced by ∼7500-fold (0.016 ± 0.004 min^{-1}). This result indicates the critical role of hydrogen bonding between matched base pairing (UTP:dA) in ensuring the rapid RNA Pol II incorporation of cognate substrate (∼7500 contribution in catalytic rate).

We further measured the respective incorporation rates for HTP, LTP, BTP and ITP. Interestingly, we found that the smaller-sized analogue HTP shows a slower incorporation rate comparing with the FTP incorporation, while the incorporation rates of the larger-sized analogues LTP and BTP are ∼50-fold higher than that of the FTP incorporation (Table 1). These results revealed that the nucleobase size is another important factor in controlling the NTP incorporation rate. Increased nucleobase size promotes stronger base stacking between incoming NTP and RNA 3′ terminus (39,40,42), which can boost catalytic efficiency. On the other hand, the maximum size of nucleobase is restricted by surrounding Pol II active site residues and the template nucleobase. As observed, the rate of ITP incorporation was reduced to almost the same level as that of the FTP incorporation. Therefore, we observed a bell-shaped kinetic profile across the five NTP analogues, reflecting a fine balance between two competing factors, nucleobase stacking and steric effects, in controlling substrate incorporation. The incorporation rates are increased from HTP to LTP and BTP incorporation apparently due to enhanced base stacking, and rates are decreased from BTP to ITP incorporation due to the steric restrictions of the Pol II active site. Interestingly, a similar trend (bell-shape) was also observed in DNA polymerase and human thymidine kinases, suggesting a common mechanism of the balancing effects of stacking interactions and steric sizes within enzyme active site (39,41,42).

Next, we investigated the effect of α-amanitin treatment on the incorporation of UTP and 'hydrogen-bond-deficient' nucleotide analogues for the matched UTP incorporation opposite dA template. α-Amanitin treatment can greatly inhibit the catalytic rate of the cognate UTP opposite to its complementary dA template (AEI = 55 ± 9), which indicates an active and closed TL during UTP incorporation (Figure 2B). This is similar to the cognate ATP incorporation opposite its matched dT template (Figure 1B). Interestingly, the AEI for the 'hydrogen-bond-deficient' FTP incorporation opposite dA template is 16, suggesting that a partially closed TL can still be achieved even in the absence of hydrogen bonding as long as the size and complementary shape remains. For the smaller-sized nucleotide analogue HTP incorporation, the AEI value is reduced. More strikingly, we observed high AEI values for larger-sized nucleotide analogues LTP (∼70) and BTP (∼130), which are comparable to the AEI of matched UTP incorporation. These results (LTP and BTP) indicate that increased size and base stacking can efficiently compensate for the loss of hydrogen bonding during base pairing and strongly pro-

Table 1. Rate constants for RNA Pol II incorporation of hydrogen-bond-deficient nucleobase analogues.

Incorporation	Substrate	k_{obs} (min^{-1})		AEI
		− α-amantin[a]	+ α-amantin[b]	
XTP:dA	UTP	120 ± 20	2.2 ± 0.1	55 ± 9
	HTP	0.010 ± 0.001	0.0008 ± 0.0001	13 ± 2
	FTP	0.016 ± 0.004	0.0010 ± 0.0001	16 ± 4
	LTP	0.8 ± 0.1	0.011 ± 0.002	68 ± 16
	BTP	0.80 ± 0.04	0.0063 ± 0.0005	130 ± 10
	ITP	0.025 ± 0.001	0.0012 ± 0.0001	20 ± 2
XTP:dT	UTP	0.023 ± 0.006	0.008 ± 0.004	3.0 ± 1.9
	HTP	0.0049 ± 0.0006	0.0024 ± 0.0003	2.0 ± 0.4
	FTP	0.013 ± 0.005	0.004 ± 0.003	3.0 ± 2.3
	LTP	0.13 ± 0.01	0.025 ± 0.008	5.2 ± 1.7
	BTP	0.13 ± 0.02	0.016 ± 0.005	8.1 ± 2.8
	ITP	0.087 ± 0.006	0.0042 ± 0.0002	21 ± 2

[a]Observed rate constants without (−) treatment of α-amanitin.
[b]Observed rate constants with (+) treatment of α-amanitin.

mote TL transition to a closed state for matched nucleotide analogue (complementary shape). Further increasing the base size would hinder nucleotide binding, as we observed the less inhibitory effect of α-amanitin for ITP incorporation (∼20-fold). Taken together, the variation in AEI values across the 'hydrogen-bond-deficient' analogues reveals a fine balance between two competing factors, base stacking and steric effects, in controlling TL conformational transition during the matched NTP incorporation. We found that while Watson–Crick hydrogen bonds between nucleotide and its template play a very important role in ensuring efficient incorporation, their contribution to promoting TL closure is less prominent. TL can be partially closed in the absence of hydrogen bonding. For the matched NTP incorporation, the loss of hydrogen bonds can be fully compensated by increasing base stacking (LTP and BTP) in terms of promoting full TL closure and nucleotide incorporation.

To study the case of nucleotide misincorporation, we substituted the +1 position of DNA template from dA to dT (termed dT template, mismatch for UTP incorporation), so it allows us to use the same set of nucleotide triphosphate substrates for a direct comparison of two scenarios. We measured the incorporation rates of UTP, HTP, FTP, LTP, BTP and ITP opposite a mismatched dT template (non-complementary shape) (Figure 2C and Table 1). For canonical UTP, the incorporation rate opposite the mismatched dT template slows down by ∼5000-fold in comparison to its incorporation opposite the matched dA template (Figure 2B, C). In sharp contrast, for the 'hydrogen-bond-deficient' FTP, the incorporation rate of FTP opposite the mismatched dT template is comparable to its incorporation to the matched dA template (Figure 2B, C). Similarly, the incorporation rates for these analogues opposite dT template increased when the nucleobase size is increased from HTP, FTP to LTP and BTP and slightly decreased when the nucleobase size is further increased from BTP to ITP (Figure 2C).

Finally, we investigated the effect of α-amanitin treatment on the respective incorporation rates of UTP, HTP, FTP, LTP, BTP and ITP opposite dT template. We found that AEI value is ∼3 for mismatched UTP incorporation opposite dT template (Figure 2C). These low AEI values are consistent with previous structural and biochemical studies that the major binding site of mismatched nucleotide is the entry site and TL remains at an open conformation for mismatched nucleotide incorporation. For the hydrogen-bond-deficient analogue FTP, AEI remains as 3, suggesting that TL remains at an open conformation in the absence of hydrogen bond capacity. Indeed, the entry site for mismatched nucleotide binding does not require hydrogen bond formation with template base. We also compared AEI values of all five hydrogen-bond-deficient analogues (HTP, FTP, LTP, BTP and ITP) (Figure 2C). Interestingly, the AEI values increased from 2 to 21 when the nucleobase size changed from HTP to ITP. These results suggest that the dominant state of TL is changed from an open state (HTP, FTP) to a partially closed TL state (ITP) during mismatched nucleotide incorporation. The increase of nucleobase size may shift the nucleotides from entry site to approximate canonical addition site to allow partial closure of TL.

Dominant contributions of sugar pucker in TL-dependent transcription

Pol II has a strong sugar discrimination of ribonucleotide over deoxyribonucleotide. The difference observed between dATP and ATP in Pol II enzymatic efficiency is attributed by the combination of these two factors: 2′-OH interaction and sugar ring conformation. First, 2′-OH forms hydrogen bonding interactions with Pol II residues in which the loss of intact 2′-OH results in the disruption of this hydrogen bonding network and may affect TL conformational transition. Second, the loss of 2′-OH leads to the sugar pucker conformational change from a dominant C3′-endo conformation to a C2′-endo conformation.

In order to dissect the individual contribution of these two factors, we employed two ATP analogues: unlocked ATP (UNA-ATP) and locked ATP (LNA-ATP) (Figure 3A) (24,35,43–46). UNA-ATP is a nucleic acid analogue consisting of all of the functional groups of natural NTP but lacking a bond between C2 and C3 in the sugar ring. As a result, the conformation of sugar ring in UNA is more flexible than the favored C3′-endo conformation in NTP even though it contains an intact 2′-OH group. In contrast, LNA is a nucleotide that has a well-restrained C3′-endo

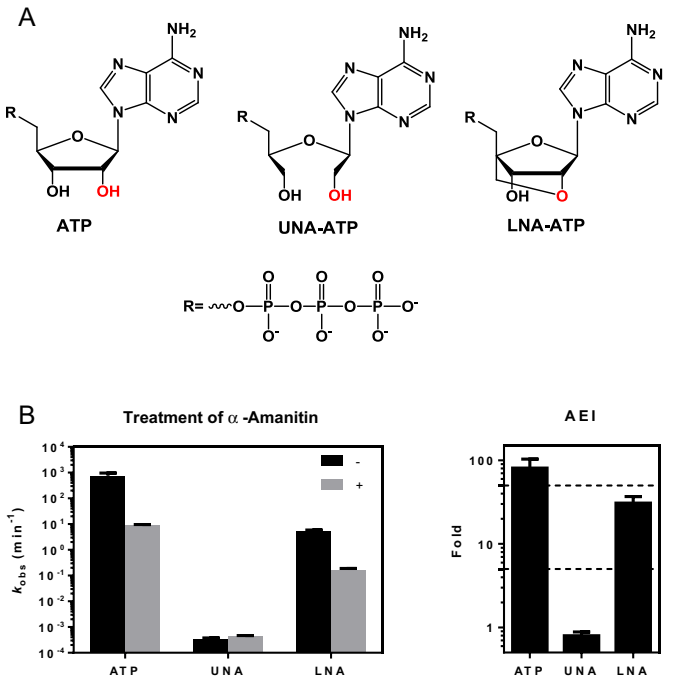

Figure 3. Sugar alteration reveals a dominant contribution of sugar conformation to efficient nucleotide incorporation and TL recognition. (A) Locked and unlocked nucleotides (UNA and LNA). The major difference between UNA and LNA is the sugar conformation and 2′-OH. (B) Incorporation rates of UNA and LNA and the effect of α-amanitin. The left panel presents observed rates in the absence (−) and presence (+) of α-amanitin; the right panel presents α-amanitin effect index.

conformation but lacks an intact 2′-OH functional group. UNA and LNA have been widely used as RNA mimics. The overall geometries of the RNA single strand and helix are not significantly affected by the replacement of UNA, and UNA can still form Watson–Crick base pairs with RNA (44,45,47). Nuclear magnetic resonance and X-ray structural studies both showed that the LNA:RNA duplex and LNA:LNA duplex adopt A-type helix (48–50). These previous studies showed that both UNA and LNA have limited effect on base pairing and stacking in nucleic acid structures, which indicates that they are suitable for investigating the contribution of sugar. Here we measured the incorporation rates for two nucleotide analogues: UNA-ATP and LNA-ATP incorporations (opposite to matched dT template) (Figure 3B and Table 2). UNA-ATP contains intact 2′-OH and 3′-OH but lacks an intact sugar ring, whereas LNA-ATP maintains the same sugar pucker conformation as the ribonucleotide but lacks an intact 2′-OH.

Strikingly, the observed UNA-ATP incorporation rate (~0.00035 min^{-1}) was significantly lower than the wild-type ATP incorporation rate with a ~10^6-fold decrease. On the other hand, the LNA-ATP incorporation (~5.1 min^{-1}) was only moderately reduced by ~100-fold (Figure 3B). The comparison of UNA-ATP and LNA-ATP with ATP incorporation implies different contributions of 2′-OH interaction and sugar ring conformation. Maintaining intact 2′-OH but lacking a C3′-endo sugar conformation in UNA-ATP resulted in a substantial decrease in incorporation rate, reflecting a dominant role of sugar ring conformation in NTP incorporation as we have previously reported (35). In contrast, maintaining a C3′-endo sugar conformation but lacking an intact 2′-OH as shown in LNA-ATP only caused moderate decrease in incorporation rate, indicating that while the intact 2′-OH can affect enzymatic activity, it is not as critical as the sugar ring conformation.

To further investigate the involvement of TL in sugar discrimination, AEI values were determined for ATP, UNA-ATP and LNA-ATP, respectively. As shown in Figure 3B, the treatment of α-amanitin did not change the incorporation rate of UNA-ATP, indicating an inactive open TL during UNA-ATP incorporation. In contrast, LNA-ATP incorporation was greatly inhibited by α-amanitin with an AEI value over 30. This AEI value implies a partially closed TL during LNA-ATP incorporation. Taken together, these results clearly showed that the TL cannot recognize the flexible sugar ring conformation even in the presence of all of the functional groups, while a correct C3′-endo conformation is more important for promoting TL transition to a closed state.

DISCUSSION

Employing a combination of synthetic nucleotide analogues and α-amanitin inhibition assays, we assessed the individual contributions of key chemical interactions and structural signatures of NTP governing the TL-dependent substrate recognition and TL closure. Our results unravel the unexpected roles of these interactions during TL-dependent NTP incorporation.

First, our data suggest that the formation of Watson–Crick hydrogen bonds is dispensable to promoting TL closure, and the loss of hydrogen bonds can be fully rescued by increasing the size (base stacking) of a nucleobase. The replacement of natural UTP by hydrogen-bond-deficient LTP or BTP does not alter the TL closure behavior, as evidenced by similar effect of α-amanitin treatment. The AEIs of 'hydrogen-bond-deficient' analogues LTP and BTP are either similar or higher than the canonical UTP incorporation (Figure 2B), suggesting that a full closure of TL can be achieved even in the absence of Watson–Crick hydrogen bonds. This result demonstrates that the loss of hydrogen bonds in base pairing is not critical for TL closure, and Pol II can still recognize the substrate and close its TL even in the absence of hydrogen bonds during base pairing.

Further comparative analysis among these hydrogen-bond-deficient nucleotides (HTP, FTP, LTP, BTP and ITP) also reveals important contributions of base stacking and size matching for the TL closure. Varying size from HTP to ITP, the TL underwent partial closure to full closure and back to partial closure again for complementary dA template. This variation was attributed by a combination of base stacking and steric size effect. From HTP to BTP, the base stacking was increased (40) while the size change is still tolerable for the incorporation site and thus resulting in TL closure. These results reveal that increased base stacking can efficiently compensate for the loss of hydrogen bonding during base pairing. However, when incorporating ITP, the oversized nucleobase is unable to match the limited active site, which caused a partially closed TL. It is intriguing to note that the Pol II active site is able to dis-

Table 2. Rate constants for RNA Pol II incorporation of ribose ring analogues.

Substrate	k_{obs} (min^{-1})		AEI
	− α-amantin[a]	+ α-amantin[b]	
ATP	750 ± 210	9.3 ± 0.4	81 ± 23
UNA-ATP	0.00035 ± 0.00003	0.00044 ± 0.00003	0.80 ± 0.09
LNA-ATP	5.1 ± 0.7	0.17 ± 0.02	31 ± 6

[a]Observed rate constants without (−) treatment of α-amanitin.
[b]Observed rate constants with (+) treatment of α-amanitin.

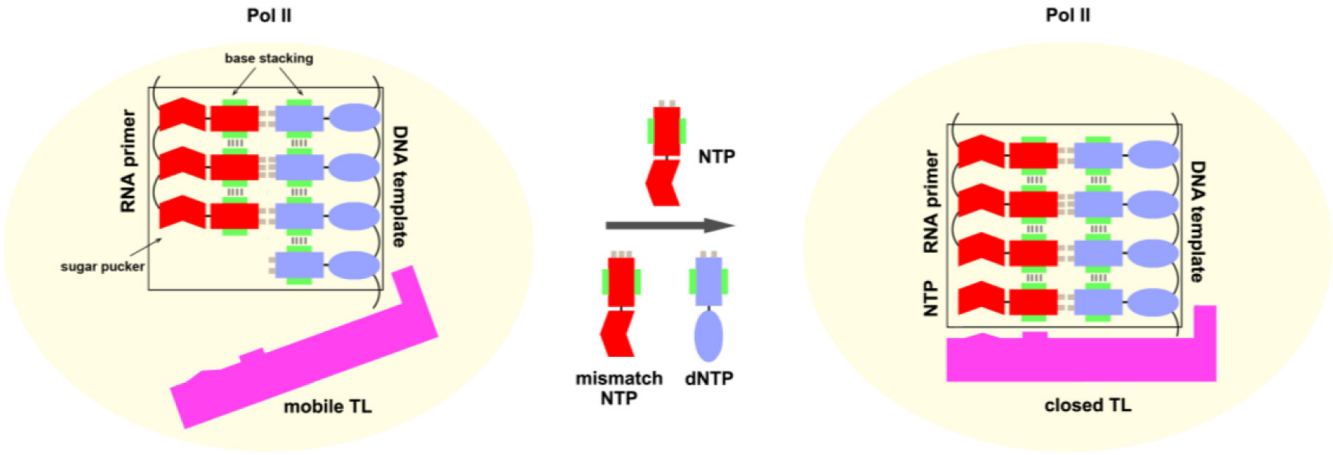

Figure 4. Strong base stacking and suitable sugar pucker are two key factors governing RNA Pol II TL closure. The DNA, RNA, and trigger loop are shown in blue, red, and magenta, respectively. The rest of Pol II is shown as a pale yellow oval. The active site is shown in the box. The base stacking is highlighted in green rectangle. Hydrogen bonds between base pairs are shown in gray.

tinguish the subtle size differences between these analogues (less than 1.0 Å). Taken together, the TL can still well recognize hydrogen-bond-deficient nucleotides with increased base stacking, and it is also very sensitive to the base size and shape.

Second, the sugar pucker ring conformation plays a much more important role in facilitating nucleotide incorporation and TL closure than that of hydrogen bonds via 2′-OH. Previous studies showed that the main cause of observed difference in discriminating NTP over dNTP is the loss of hydrogen bonds between 2′-OH and Pol II residues, including the TL. Here we revealed a dominant role of the sugar pucker ring conformation in nucleotide incorporation and TL recognition, which is underappreciated. Comparing the UNA-ATP (with all of the functional groups and in the absence of a constrained sugar ring) and LNA-ATP (with correct sugar pucker ring conformation and in the absence of intact 2′-OH) analogues with canonical ATP, we concluded that the correct sugar ring conformation, rather than hydrogen bonds, is more critical for RNA Pol II substrate incorporation and TL closure.

In summary, here we revealed that the TL closure upon substrate binding is controlled by multiple chemical interactions including hydrogen bonding, π-π base stacking and van der Waals interactions (Figure 4). Intriguingly, we showed that the contributions of hydrogen bonds between base pairs and 2′-OH with Pol II residues to TL closure are dispensable. Our studies highlighted the important, perhaps underappreciated, contributions of π-π stacking (base stacking) and van der Waals interactions (sugar pucker) governing the Pol II substrate recognition and full TL closure. Our synthetic chemical biology approach allows us to gain new insights that could not be achieved by conventional biology observations and analyses (26,30,32). This approach can provide a novel perspective in understanding the mechanisms of nucleic acid enzymes.

ACKNOWLEDGMENT

We thank Dr. E. Peter Geiduschek for critical readings of our manuscript.

FUNDING

National Institutes of Health (NIH) [GM102362 to D.W., GM072705 and GM068122 to E.T.K.]; Sidney Kimmel Foundation for Cancer Research [Kimmel Scholar Award to D.W.]; Skaggs School of Pharmacy and Pharmaceutical Sciences, UCSD [D.W.]. European Research Council [FP7/2007-2013)/ERC grant agreement No. 268776 to J.W.]. Funding for open access charge: NIH.

REFERENCES

1. Liu,X., Bushnell,D.A. and Kornberg,R.D. (2013) RNA polymerase II transcription: structure and mechanism. *Biochim. Biophys. Acta*, **1829**, 2–8.
2. Su Zhang,D.W. (2013) Understanding the molecular basis of RNA polymerase II transcription. *Isr. J. Chem.*, **53**, 442–449.
3. Svetlov,V. and Nudler,E. (2013) Basic mechanism of transcription by RNA polymerase II. *Biochim. Biophys. Acta*, **1829**, 20–28.

4. Reines,D., Conaway,R.C. and Conaway,J.W. (1999) Mechanism and regulation of transcriptional elongation by RNA polymerase II. *Curr. Opin. Cell Biol.*, **11**, 342–346.
5. Cheung,A.C. and Cramer,P. (2012) A movie of RNA polymerase II transcription. *Cell*, **149**, 1431–1437.
6. Yuzenkova,Y., Bochkareva,A., Tadigotla,V.R., Roghanian,M., Zorov,S., Severinov,K. and Zenkin,N. (2010) Stepwise mechanism for transcription fidelity. *BMC Biol.*, **8**, 54.
7. Brueckner,F., Ortiz,J. and Cramer,P. (2009) A movie of the RNA polymerase nucleotide addition cycle. *Curr. Opin. Struct. Biol.*, **19**, 294–299.
8. Wang,D., Bushnell,D.A., Westover,K.D., Kaplan,C.D. and Kornberg,R.D. (2006) Structural basis of transcription: role of the trigger loop in substrate specificity and catalysis. *Cell*, **127**, 941–954.
9. Kaplan,C.D., Larsson,K.-M. and Kornberg,R.D. (2008) The RNA polymerase II trigger loop functions in substrate selection and is directly targeted by alpha-amanitin. *Mol. Cell*, **30**, 547–556.
10. Kireeva,M.L., Nedialkov,Y.A., Cremona,G.H., Purtov,Y.A., Lubkowska,L., Malagon,F., Burton,Z.F., Strathern,J.N. and Kashlev,M. (2008) Transient reversal of RNA polymerase II active site closing controls fidelity of transcription elongation. *Mol. Cell*, **30**, 557–566.
11. Toulokhonov,I., Zhang,J., Palangat,M. and Landick,R. (2007) A central role of the RNA polymerase trigger loop in active-site rearrangement during transcriptional pausing. *Mol. Cell*, **27**, 406–419.
12. Larson,M.H., Zhou,J., Kaplan,C.D., Palangat,M., Kornberg,R.D., Landick,R. and Block,S.M. (2012) Trigger loop dynamics mediate the balance between the transcriptional fidelity and speed of RNA polymerase II. *Proc. Natl. Acad. Sci. U.S.A.*, **109**, 6555–6560.
13. Huang,X., Wang,D., Weiss,D.R., Bushnell,D.A., Kornberg,R.D. and Levitt,M. (2010) RNA polymerase II trigger loop residues stabilize and position the incoming nucleotide triphosphate in transcription. *Proc. Natl. Acad. Sci. U.S.A.*, **107**, 15745–15750.
14. Feig,M. and Burton,Z.F. (2010) RNA polymerase II with open and closed trigger loops: active site dynamics and nucleic acid translocation. *Biophys. J.*, **99**, 2577–2586.
15. Zhang,J., Palangat,M. and Landick,R. (2010) Role of the RNA polymerase trigger loop in catalysis and pausing. *Nat. Struct. Mol. Biol.*, **17**, 99–104.
16. Kettenberger,H., Armache,K.-J. and Cramer,P. (2004) Complete RNA polymerase II elongation complex structure and its interactions with NTP and TFIIS. *Mol. Cell*, **16**, 955–965.
17. Westover,K.D., Bushnell,D.A. and Kornberg,R.D. (2004) Structural basis of transcription: nucleotide selection by rotation in the RNA polymerase II active center. *Cell*, **119**, 481–489.
18. Batada,N.N., Westover,K.D., Bushnell,D.A., Levitt,M. and Kornberg,R.D. (2004) Diffusion of nucleoside triphosphates and role of the entry site to the RNA polymerase II active center. *Proc. Natl. Acad. Sci. U.S.A.*, **101**, 17361–17364.
19. Da,L.T., Wang,D. and Huang,X. (2012) Dynamics of pyrophosphate ion release and its coupled trigger loop motion from closed to open state in RNA polymerase II. *J. Am. Chem. Soc.*, **134**, 2399–2406.
20. Brueckner,F. and Cramer,P. (2008) Structural basis of transcription inhibition by alpha-amanitin and implications for RNA polymerase II translocation. *Nat. Struct. Mol. Biol.*, **15**, 811–818.
21. Bushnell,D.A., Cramer,P. and Kornberg,R.D. (2002) Structural basis of transcription: alpha-amanitin-RNA polymerase II cocrystal at 2.8 A resolution. *Proc. Natl. Acad. Sci. U.S.A.*, **99**, 1218–1222.
22. Svetlov,V., Vassylyev,D.G. and Artsimovitch,I. (2004) Discrimination against deoxyribonucleotide substrates by bacterial RNA polymerase. *J. Biol. Chem.*, **279**, 38087–38090.
23. Huang,Y., Eckstein,F., Padilla,R. and Sousa,R. (1997) Mechanism of ribose 2′-group discrimination by an RNA polymerase. *Biochemistry*, **36**, 8231–8242.
24. Campbell,M.A. and Wengel,J. (2011) Locked vs. unlocked nucleic acids (LNA vs. UNA): contrasting structures work towards common therapeutic goals. *Chem. Soc. Rev.*, **40**, 5680–5689.
25. Banfalvi,G. (2006) Why ribose was selected as the sugar component of nucleic acids. *DNA Cell. Biol.*, **25**, 189–196.
26. Khakshoor,O. and Kool,E.T. (2011) Chemistry of nucleic acids: impacts in multiple fields. *Chem. Commun. (Camb)*, **47**, 7018–7024.
27. Benner,S.A. (2004) Chemistry. Redesigning genetics. *Science*, **306**, 625–626.
28. Opalinska,J.B. and Gewirtz,A.M. (2002) Nucleic-acid therapeutics: basic principles and recent applications. *Nat. Rev. Drug Discov.*, **1**, 503–514.
29. Steele,F.R. and Gold,L. (2012) The sweet allure of XNA. *Nat. Biotechnol.*, **30**, 624–625.
30. Benner,S.A. and Sismour,A.M. (2005) Synthetic biology. *Nat. Rev. Genet.*, **6**, 533–543.
31. Pinheiro,V.B., Taylor,A.I., Cozens,C., Abramov,M., Renders,M., Zhang,S., Chaput,J.C., Wengel,J., Peak-Chew,S.Y., McLaughlin,S.H. *et al.* (2012) Synthetic genetic polymers capable of heredity and evolution. *Science*, **336**, 341–344.
32. Benner,S.A. (2004) Understanding Nucleic Acids Using Synthetic Chemistry. *Acc. Chem. Res.*, **37**, 784–797.
33. Chaput,J.C., Yu,H. and Zhang,S. (2012) The emerging world of synthetic genetics. *Chem. Biol.*, **19**, 1360–1371.
34. Kellinger,M.W., Ulrich,S., Chong,J., Kool,E.T. and Wang,D. (2012) Dissecting chemical interactions governing RNA polymerase II transcriptional fidelity. *J. Am. Chem. Soc.*, **134**, 8231–8240.
35. Xu,L., Plouffe,S.W., Chong,J., Wengel,J. and Wang,D. (2013) A chemical perspective on transcriptional fidelity: dominant contributions of sugar integrity revealed by unlocked nucleic acids. *Angew. Chem. Int. Ed. Engl.*, **52**, 12341–12345.
36. Wang,D., Bushnell,D.A., Huang,X., Westover,K.D., Levitt,M. and Kornberg,R.D. (2009) Structural basis of transcription: backtracked RNA polymerase II at 3.4 angstrom resolution. *Science*, **324**, 1203–1206.
37. Kellinger,M.W., Song,C.X., Chong,J., Lu,X.Y., He,C. and Wang,D. (2012) 5-formylcytosine and 5-carboxylcytosine reduce the rate and substrate specificity of RNA polymerase II transcription. *Nat. Struct. Mol. Biol.*, **19**, 831–833.
38. Attwater,J., Tagami,S., Kimoto,M., Butler,K., Kool,E.T., Wengel,J., Herdewijn,P., Hiraob,I. and Holliger,P. (2013) Chemical fidelity of an RNA polymerase ribozyme. *Chem. Sci.*, **4**, 2804–2814.
39. Kim,T.W., Delaney,J.C., Essigmann,J.M. and Kool,E.T. (2005) Probing the active site tightness of DNA polymerase in subangstrom increments. *Proc. Natl. Acad. Sci. U.S.A.*, **102**, 15803–15808.
40. Kim,T.W. and Kool,E.T. (2005) A series of nonpolar thymidine analogues of increasing size: DNA base pairing and stacking properties. *J. Org. Chem.*, **70**, 2048–2053.
41. Jarchow-Choy,S.K., Sjuvarsson,E., Sintim,H.O., Eriksson,S. and Kool,E.T. (2009) Nonpolar nucleoside mimics as active substrates for human thymidine kinases. *J. Am. Chem. Soc.*, **131**, 5488–5494.
42. Krueger,A.T. and Kool,E.T. (2007) Model systems for understanding DNA base pairing. *Curr. Opin. Chem. Biol.*, **11**, 588–594.
43. Jensen,T.B., Henriksen,J.R., Rasmussen,B.E., Rasmussen,L.M., Andresen,T.L., Wengel,J. and Pasternak,A. (2011) Thermodynamic and biological evaluation of a thrombin binding aptamer modified with several unlocked nucleic acid (UNA) monomers and a 2′-C-piperazino-UNA monomer. *Bioorg. Med. Chem.*, **19**, 4739–4745.
44. Pasternak,A. and Wengel,J. (2010) Thermodynamics of RNA duplexes modified with unlocked nucleic acid nucleotides. *Nucleic Acids Res.*, **38**, 6697–6706.
45. Langkjaer,N., Pasternak,A. and Wengel,J. (2009) UNA (unlocked nucleic acid): a flexible RNA mimic that allows engineering of nucleic acid duplex stability. *Bioorg Med Chem*, **17**, 5420–5425.
46. Laursen,M.B., Pakula,M.M., Gao,S., Fluiter,K., Mook,O.R., Baas,F., Langklaer,N., Wengel,S.L., Wengel,J., Kjems,J. *et al.* (2010) Utilization of unlocked nucleic acid (UNA) to enhance siRNA performance in vitro and in vivo. *Mol Biosyst*, **6**, 862–870.
47. Campbell,M.A. and Wengel,J. (2011) Locked vs. unlocked nucleic acids (LNA vs. UNA): contrasting structures work towards common therapeutic goals. *Chem Soc Rev*, **40**, 5680–5689.
48. Eichert,A., Behling,K., Betzel,C., Erdmann,V.A., Furste,J.P. and Forster,C. (2010) The crystal structure of an 'All Locked' nucleic acid duplex. *Nucleic Acids Res*, **38**, 6729–6736.
49. Nielsen,K.E., Rasmussen,J., Kumar,R., Wengel,J., Jacobsen,J.P. and Petersen,M. (2004) NMR studies of fully modified locked nucleic acid (LNA) hybrids: solution structure of an LNA:RNA hybrid and characterization of an LNA:DNA hybrid. *Bioconjug Chem.*, **15**, 449–457.
50. Petersen,M., Bondensgaard,K., Wengel,J. and Jacobsen,J.P. (2002) Locked nucleic acid (LNA) recognition of RNA: NMR solution structures of LNA:RNA hybrids. *J. Am. Chem. Soc.*, **124**, 5974–5982.